Distribution Agreement

In presenting this thesis as a partial fulfillment of the requirements for a degree from Emory University, I hereby grant to Emory University and its agents the non-exclusive license to archive, make accessible, and display my thesis in whole or in part in all forms of media, now or hereafter now, including display on the World Wide Web. I understand that I may select some access restrictions as part of the online submission of this thesis. I retain all ownership rights to the copyright of the thesis. I also retain the right to use in future works (such as articles or books) all or part of this thesis.

Signature:

_____ _____

Ye Yuan 04/14/2014

Numerical Modeling of Blood Flow in Bioresorbable Vascular Stents

By

Ye Yuan

Dr. Alessandro Veneziani
Adviser

Department of Mathematics and Computer Science

_____

Dr. Alessandro Veneziani
Adviser

_____

Dr. Michele Benzi
Committee Member

_____

Dr. Trisha M. Kesar
Committee Member

2014

Numerical Modeling of Blood Flow in Bioresorbable Vascular Stents

By

Ye Yuan

Dr. Alessandro Veneziani
Adviser

An abstract of
a thesis submitted to the Faculty of Emory College of Arts and Sciences
of Emory University in partial fulfillment
of the requirements of the degree of
Bachelor of Sciences with Honors

Department of Mathematics and Computer Science

2014

Abstract

Numerical Modeling of Blood Flow in Bioresorbable Vascular Stents

By Ye Yuan

This study focuses on the numerical simulation of blood flow in vessels with Bioresorbable Vascular Stents (BVS). BVS is a recent invention that has only been approved for clinical practices in Europe. BVS has considerable advantages over the traditional metal stents, since it is flexible and resorbable. Patients may take less medication once it is completely dissolved, for it is not a permanent implant. However, BVS also has several limitations that have caught the attention of researchers. One of these limitations, the potential formation of vortexes behind the strut, is investigated in this study.

The structure and fluid in this problem, the vessel wall and the blood flow, have complicated biomechanical properties. The vascular wall is elastic and change in length over time. The blood flow is pulsatile and features a complex rheology. In this project, the blood flow is assumed to be Newtonian fluid and the vascular wall is assumed to be rigid. Under such assumptions, Incompressible Navier-Stokes equations (INS) are implemented. The boundary conditions at the inflow end of vessel segment, at the outflow end and on the vascular wall are prescribed as patient-specific blood flow data, 'free' or so-called 'do-nothing condition', and 0, respectively.

LifeV, an open source library of algorithms and data structures for the numerical solution of partial differential equations, is then employed to solve the INS numerically. ParaView, a three-dimensional visualization tool, is used to visualize the numerical results dynamically. The variables of interest, including the pressure, the velocity and the Wall Sheer Stress (WSS) can be observed in the result figures and animations.

Based on the simulation results, the WSS is low in the vicinity of the strut but high in the region between the ring struts. This distribution pattern of the WSS suggests there is a possibility that the blood flow may be turbulent behind the strut, but no obvious circulate streamlines of blood flow are observed in the velocity streamline figures. Potential paths of continued study could include simulations with sufficiently fine meshes and having the vascular wall more involved in the study of fluid-dynamic influence from the vascular wall.

Numerical Modeling of Blood Flow in Bioresorbable Vascular Stents

By

Ye Yuan

Dr. Alessandro Veneziani
Adviser

A thesis submitted to the Faculty of Emory College of Arts and Sciences
of Emory University in partial fulfillment
of the requirements of the degree of
Bachelor of Sciences with Honors

Department of Mathematics and Computer Science

2014

Acknowledgements

I would like to acknowledge Ph.D. candidate Boyi Yang，who acted as a co-advisor on this project and spent many hours teaching me throughout this year. I would like to thank my thesis adviser, Dr. Veneziani, for offering me this great opportunity and mentoring me. I also would like to thank Dr. Benzi and Dr. Kesar for being my committee members and for their comments on my work. I appreciate the Department of Mathematics and Computer Science at Emory University as a whole for helping me explore the world of mathematics and computer science and for expanding my knowledge. Lastly, I would like to thank Emory University for providing such an interdisciplinary environment and accessible resource and fascinating opportunities for research collaboration between different fields of science.

Table of Contents

1. INTRODUCTION 1

1.1 BACKGROUND 1

1.2 CONCERNS AND LIMITATIONS 2

1.3 PRIOR STUDY 4

1.4 SUMMARY 5

2. MATHEMATICAL MODELING 6

2.1 ASSUMPTIONS REGARDING BLOOD FLOW 6

2.2 ASSUMPTIONS REGARDING THE VASCULAR WALL 8

2.3 THE FLUID EQUATIONS 10

2.4 BOUNDARY CONDITION 12

2.5 QUANTITIES OF INTEREST: THE WSS 15

3. THE NUMERICAL ENGINE 17

3.1 THE GEOMETRY AND MESHING OF THE VASCULAR WALL AND THE STENT 17

3.2 LIFEV 19

3.3 THE VISUALIZATION SOFTWARE: PARAVIEW 20

3.4 THE ENVIRONMENT IN WHICH THE COMPUTATION IS CONDUCTED 21

4. NUMERICAL TESTS 23

4.1 PROCESS 23

4.2 THE VISUALIZATION RESULTS AND INTERPRETATION 27

4.3 DISCUSSION 40

4.4 INSIGHTS 42

REFERENCE 45

Table of Figures

FIGURE 1 THE VASCULAR WALL, INFLOW AND OUTFLOW ENDS OF A CURVED VESSEL 13

FIGURE 2. (A) A GEOMETRY OF STRAIGHT VESSEL. (B) A GEOMETRY OF CURVED VESSEL 17

FIGURE 3. THE SIX TYPES OF GEOMETRY 24

FIGURE 4. PRESSURE AT THE PEAK SYSTOLE: (3.5 SECOND) 8 28

FIGURE 5. PRESSURE AT PEAK DIASTOLE: (AT 3.5 SECOND)8 29

FIGURE 6. MAGNITUDE OF VELOCITY AT THE PEAK SYSTOLE: (3.5 SECOND)8 31

FIGURE 7. MAGNITUDE OF VELOCITY AT PEAK DIASTOLE: (AT 3.9 SECOND)8 32

FIGURE 8. STREAMLINES OF VELOCITY IN CURVED AND STRAIGHT VESSELS AT STAGE 2 34

FIGURE 9. VELOCITY STREAMLINES IN STRAIGHT VESSELS: (A) AT STAGE1, (B) AT STAGE2, (C) AT STAGE 3 35

FIGURE 10. WSS AT THE PEAK SYSTOLE: (3.5 SECOND)8 37

FIGURE 11. WSS AT PEAK DIASTOLE: (AT 3.9 SECOND)8 38

FIGURE 12. SIMULATIONS WITH MESHES IN DIFFERENT QUANLITY 42

1. Introduction

1.1 Background

Stent is medical device than implanted inside the coronary vessels where the vessels are narrowed (Atherosclerosis). Typically, the vascular wall thickening and/or the accumulation of the plaques on the vascular wall can cause Atherosclerosis. (Maton 35) Metal stent has been approved and widely applied in clinical practice for the treatment of this disease.

Although the development of the metal stent has been a milestone in the treatment of coronary disease, a permanent implant of a metallic device in the coronary vessel brings up concerns of delayed healing and very late stent thrombosis. Additionally, a metal stent may straighten a curved coronary segment, which may cause a troublesome biomechanical impact on the edges of the stent (McDaniel and Samady 800).

A novel approach to the treatment of coronary disease, the use of the bioresorbable stent may bring potential advantages over the use of traditional metal stents. The Absorb™ Bioresorbable Vascular Scaffold (BVS) is the only bioresorbable platform approved for clinical

use in Europe. The bioresorbable stent is made of semi-crystalline polymer, namely poly-L-lactic acid (PLLA). (Abbott, "Absorb Bioresorbable Vascular Scaffold") that is known to completely resorb over a 2-to-3-year period. It is relatively flexible and it leaves the vessel treated without a permanent implant. Insights from the ABSORB Cohort B trial suggest that BVS results in less vascular straightening and greater retention of the original angulation and curvature than metal stents. (Gogas, Bill D., Alessandro Veneziani, et al 761). Retaining natural vessel function may improve the long-term experience for the patients. Also, less oral medication may be applied after deployment and no second surgery is needed to remove the stent (Abbott, "Absorb Bioresorbable Vascular Scaffold").

1.2 Concerns and Limitations

However, despite the clear medical advantages of the BVS, this medical device has two main limitations. Firstly, the polymeric struts[1] of the BSV are thicker[2] (Gogas, Bill D., Alessandro

[1] Strut: the rings and the beams between each pair of rings

[2] The thickness of the BVS strut: 0.15 mm

[3] The thickness of the metallic strut: 0.09 mm

[4] http://sourceforge.net/projects/netgen-mesher/

Veneziani, et al 761) than those of the metallic ones[3] (Abbott, "Absorb Bioresorbable Vascular Scaffold"). Thicker struts may cause potential formation of vortexes behind the strut. Consequently, the vascular wall experience more pressure, which makes it vulnerable. In this case, the relatively thicker structure of BVS may significantly influence the fluid dynamics of the blood fluid, especially the Wall Shear Stress (WSS), an indicator introduced by fluid mechanic. Hence, WSS would be a numerical value of interest in the study of potential formation of vortexes effect.

Secondly, as the stent decomposes, the impact by blood flow may change over time. There is a possibility that as the device dissolves, the effect of preventing the vessel from narrowing may be compromised. Especially in case that the plaques grow back to the segment of vascular wall where the stent is places, the semi-resorbed stent might not be able to provide the demanded strength. Hence, to plant BVS might not meet the desired result of treatment in some cases.

Due to thesis concerns, the BVS has not been approved for clinical use outside of Europe. Studies involving numerical analysis, image processing, and other methodologies are needed for

[2] The thickness of the BVS strut: 0.15 mm

[3] The thickness of the metallic strut: 0.09 mm

resolving such issues.

1.3 Prior study

BVS is a cutting-edge technology and still in its developing stage, especially outside of Europe. Europe is so far the only area where BVS is approved for clinical usage, where the application of BVS is relatively more established.

Relevant prior studies in this specific matter of BVS are very limited. Prior to this project, Dr. Veneziani, PhD candidate Boyi Yang in Emory University, and his collaborators made great contributions to the visualization of the stents in the vessel in different stages of decomposition. Yang has simulated the static scene of blood flow in ideal and patient-specific cases of blood vessels with stents in different degree of decomposition. His work also covered the past-analysis of the simulation result, generating the velocity (including the stream lines passing the vicinity of the stent), pressure and WSS. The meshes in Yang's work are much finer than those employed in this project. Moreover, the blood flow rate (BFR) is selected to approach the human maximum BFR, which allows one observe the simulation of influence from the blood flow in an extreme.

1.4 Summary

Despite the progress in simulation of BVS in ideal and patient-specific cases in literature, overall insufficient amount of work in simulation for BVS has been done, in neither fluid- nor structure-wise. Although this project covers two styles of blood vessels, it more concentrates on studying the fluid dynamics. It adapts the geometry from Yang's work and employee patient-specific data for the blood flow to simulate it in dynamic fashion. Instead of focusing on instance as the prior studies did, this dynamic simulation offers a clearer picture of fluid dynamics in duration. Potentially, it might yield more insights in fluid dynamics of blood flow and answer relevant questions more precisely, including but not limited to the potential formation of vortexes in the vicinity of BVS rings and struts.

2. Mathematical modeling

Today, computational fluid dynamics (CFD) is a popular tool for investigating blood flow problems. It has been intensively applied in many cardiology studies, including but not limited to the physiopathology of the cardiovascular system (Ruth <page number>) and the biomechanical effects of stents (Gogas, Bill D., Alessandro Veneziani, et al 761). The computational approach includes the mathematical models and the numerical model, illustrated in the following sections.

2.1 Assumptions regarding Blood Flow

Blood is a complex suspension of plasma and different particles, including red cells (*erthrocytes*), white cells (*leukocytes*), and platelets (*thromboytes*) (Veneziani 33). Blood plasma is the pale-yellow liquid component of blood that normally holds the blood cells in suspension. It makes up about 55% of the body's total blood volume (O'Neil 1). Blood plasma can be considered Newtonian fluid.

The two most significant features of blood flow in arteries concerning this study’s

mathematical models are blood flow pulsatility and rheology. Pulsatility is the contractive and relaxing motion of the heart that induces pressure differences, creating waves of pressure and instigating blood flow. Rheology is the study of the flow of fluid under conditions in which they respond with flow rather than deforming elastically in response to an applied force (Schowalter 277). Rheology of blood is related to its component. Red cells are considerably large and influence the rheological behavior of the blood. One of the most important characteristics of blood flow rheology is Shear Thinning Behavior (STB). If we denote the ratio of shear stress (force) and the rate of deformation (apparent viscosity) as r, STB refers to the relationship between the shear rate and r, that is, the ratio r decreases as the shear rate increases (Veneziani 36). Explained more simply, the viscosity (which, in the case of blood, corresponds to the notion of "thickness") drops as more blood is agitated. The thinner the blood gets as the faster it flows.

However, in the model of this project, the features of blood flow are simplified. The rheology feature can be neglected, since the vessels studied in this project are sufficiently large. Therefore, the viscosity of the blood is assumed to be constant in this project, which means the blood may behave like Newtonian fluid. A fluid is Newtonian if the non-isotropic parts of the

stress are linearly proportional to the rate-of-strain tensor (Batchelor 146). Here, the non-isotropic parts of the stress refer to the parts that can be attributed to the strain rate.

Hence, blood flow would be considered incompressible Newtonian fluid with constant viscosity. The incompressible fluid can be interpreted as the fluid with constant density.

2.2 Assumptions regarding the vascular wall

The blood vascular walls consist of three layers, the innermost tunica (intima), the tunica media, and the outmost tunica (Adventitia) (Pedley80).

There are three common assumptions in this project, based on the experimental evidence that (Skalak 87)(Fung 620):

(1) The vessel has a cylindrical structure;

(2) The vascular wall is incompressible;

(3) Deformations are orthotropic.

The cylindrical structure and the *orthotropy* imply that the vessel could be simulated as an ordinary cylinder. The incompressibility suggests that one can consider the vascular wall a

structure with constant volume and density (Veneziani 51).

The features of the vascular wall include its static and dynamic properties. The blood vessels undergo the cyclic loading and unloading stages, corresponding to the contractive and relaxing motions of the heart. The large- and medium-sized arteries, including aorta, succlavian, carotid, iliac, cerebral and renal arteries, are elastic (Veneziani 52). One of the most notable static properties of the vascular wall is its longitudinal behavior. During cardiac cycles, the length of the vessel would change.

However, it is common for the researchers not to take the longitudinal changes in most types of vessels (make a foot note: The only exception are the ascending aorta and the pulmonary arteries that changes in length up to 11% because of the overall motion of heart during rapid ventricular ejection) into consideration in simulations, due to the presence of “perivascular” connective tissue (Veneziani 52). Perivascular connective tissue can be briefly described as the longest and thickest connective tissue found in the vicinity of the stronger venous and arterial circulation systems (Ciechanowski 48).

One of the important dynamic properties of the blood vessels is the strain-rate insensitivity

of the hysteretic loop. The strain rate in this project describes the change of deformation of vessels over time. The hysteretic loop in this case, H, refers to the ratio between the area of the loop in one cardiac cycle and the area under the loading part of the. It is obvious from the graph that the frequency of the loading-and-unloading cycle is not one of the contributors upon which the hysteretic loop depends. Hence, the hysteretic loop is not sensitive to the strain rate, either, as the strain rate is subjected to time (Veneziani 54).

In this project, the longitudinal change is neglected, as researchers often do for mathematical models of vascular walls. “No slip” condition is also assumed on the vascular wall. “No slip” refers to that the blood in contact with the vascular wall has speed zero. Literally, the blood is not slipping on the vascular wall. The three assumptions regarding vascular walls are also employed. Moreover, the vascular walls are assumed to be rigid for the purpose of simplifying the model. In the big picture, the blood vessel in the model of this project is analogous to cylindrical pipes that are infinite, rigid, and hollow.

2.3 The Fluid equations

In this project, the blood flow is considered as incompressible fluid. The motion of blood

flow over a time interval is described by the Incompressible Navier-Stokes (INS) equations:

$$\rho \frac{\partial \boldsymbol{u}}{\partial t} + \rho(\boldsymbol{u} \cdot \nabla)\boldsymbol{u} - \mu \Delta \boldsymbol{u} + \nabla p = f$$

$$\nabla \cdot \boldsymbol{u} = 0$$

ρ is the fluid density, $\mathbf{u}$ is the fluid velocity, t is the time, ∇ is the first-order partial derivative operator, Δ is the second-order partial derivative operator, μ is the fluid dynamic viscosity and f is the body force (external force, which includes gravity).

Since we consider the blood flow as Newtonian fluid, it satisfies mass conservation and Newton's Second Law of Motion, $\boldsymbol{F} = m \cdot \boldsymbol{a}$, where $\boldsymbol{F}$ is the force, m is the mass and $\boldsymbol{a}$ is the acceleration. For one volume-wise unit of fluid, the mass is mass per unit, which is fluid density ρ. The forces one needs to take into considerations are the resistance of flowing, the pressure and the body forces. The resistance of flowing can be presented $\mu \Delta \boldsymbol{u}$, the pressure can be presented by ∇p, and sum of the body forces can be presented as f. The sum of all the forces is $\mu \Delta \boldsymbol{u} - \nabla p + f$. Because the equation is for one unit of the fluid, which is a portion of the material of interest, material derivative is employed to indicate the acceleration, $\frac{\partial \boldsymbol{u}}{\partial t} + (\boldsymbol{u} \cdot \nabla)\boldsymbol{u}$. Put all the quantities into the equation of Newton's Second Law of Motion, we have

$\mu\Delta\boldsymbol{u} - \nabla p + f = \rho[\frac{\partial \boldsymbol{u}}{\partial t} + (\boldsymbol{u} \cdot \nabla)\boldsymbol{u}]$, which transfers to the form of Navier-Stokes equation as above.

In our problem, we focus on blood flow in a vessel, so it is commonly acceptable to ignore the body force (Galdi 43).

2.4 boundary condition

The boundary condition is prescribed on the vascular wall and the inflow and outflow ends of the vessel. The boundary on the two ends of the vessel is often addressed as the "artificial boundary", since there is no physical interface. The two ends are used to separate the part of interest (see Figure 1).

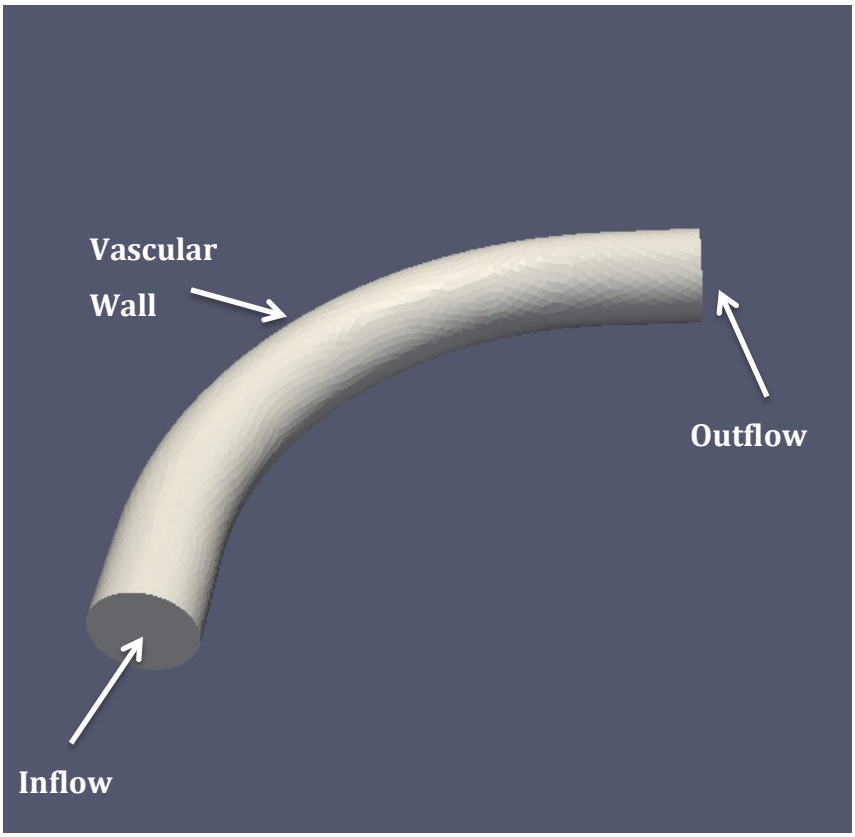

Figure 1 The vascular wall, inflow and outflow ends of a curved vessel

During the contractive motion of the heart, the blood in the large vessel is pumped towards the section of vessel being studied. The boundary condition on the inflow end of the vessel is prescribed based on the flow rate $Q(t)$, which is based on patient-specific data. Hence,

$$\rho \int \boldsymbol{u}(t)\boldsymbol{n} = Q(t)$$

$\boldsymbol{u}$ is the blood flow velocity, $\boldsymbol{n}$ is the normal unit vector, and ρ is the fluid density. $\boldsymbol{u}$ can be expressed as:

$$\boldsymbol{u} = g(\boldsymbol{x}) \cdot T(t)$$

$T(t)$ is a function depending on time t and $g(\boldsymbol{x})$ is the function depending on position, which is often given. $T(t)$ is selected to satisfy that

$$\rho T(t) \int g(\boldsymbol{x}) \cdot \boldsymbol{n} = Q(t)$$

$$T(t) = \frac{Q(t)}{\rho \int g(\boldsymbol{x}) \cdot \boldsymbol{n}}$$

Blood then flows out from outflow end of the section. The boundary condition on the output end is set to be 'free':

$$p \cdot n - \nu(\nabla u + \nabla u^T)n = 0$$

p is the pressure, n is the unit vector normal to the wall, u is the fluid velocity, and ν is the fluid viscosity.

The boundary condition on the vascular wall corresponds to a *non-slip condition* for blood particles. *Non-slip condition* allows one to prescribe that the blood in contact with the wall is not slipping on the vascular wall. The vessel is assumed to be rigid. The boundary condition on the vascular wall is prescribed as (homogeneous Dirichlet condition):

$$\mathbf{u}(\mathrm{t}, \mathbf{x}) = \mathbf{0}$$

x is a point on the vascular wall and t is time.

2.5 Quantities of Interest: the WSS

One of the goals in this project is to classify the influence of the stent applied to the blood flow. To quantify how blood flow influences the vascular wall, one important numerical method to be taken into consideration is Wall Shear Stress (WSS).

WSS is the tangential component of the normal stress (force) on the vascular wall, that is, the normal stress per unit of area of the wall. WSS is applied by the blood flow onto the vascular wall. In this project, it is defined numerically as:

$$WSS = -\nu(\nabla u + \nabla u^T)n + \nu[n^T(\nabla \mathrm{u} + \nabla \mathrm{u}^T)n]n$$

n is the unit vector normal to the wall, u is the fluid velocity, and ν is the fluid viscosity.

WSS can be an important numerical indicator of the stent conformability. Improved coronary WSS illustrates the benefit of increased stent conformability. Based on the experimental and clinical studies, low WSS is shown to promote atherosclerosis and plague progression in native arteries (Eshtehardi 236)(Stone) and greater intimal hyperplasia after stent deployment (Papafaklis 1181)(Wentzel 1740).

Metallic stents deployed in a curved vessel were noted to cause straightening in the stent segment of the vessel and increased curvature at the stent edges. Insights from computational fluid dynamics simulations done in the past suggest that the dramatic change of mechanic characteristics in the vicinity of the stent edges may induce sites of pressure wave reflection and large-scale flow disturbance (McDaniel 801). The raised curvature increases the maximum and decreases the minimum of WSS values around the stent edges. It also lowers the WSS in the in-stent segment of blood vessel. Theoretically, these drawbacks of the metallic stents can be largely eliminated by BVS. Detailed study of WSS regarding BVS in straight and curved vessels will be demonstrated later in the result section.

3. The numerical Engine

3.1 The Geometry and Meshing of the Vascular Wall and the Stent

In this project, we study two types of the vascular walls, the straight vessel and the curved. Thus, the geometries of the vascular wall are regular cylinders in the two shapes. (See Figure 2) The inflow end of the vessel is the constructed in the same size as the outflow end.

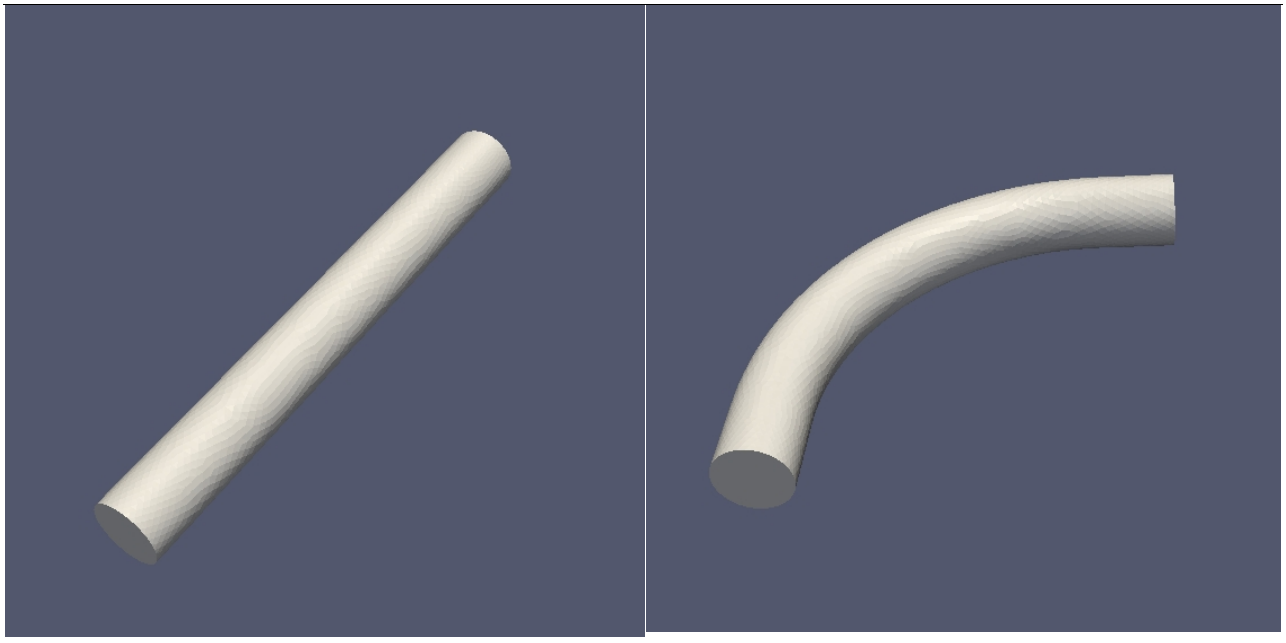

(a) (b)

Figure 2. (a) a geometry of straight vessel. (b) a geometry of curved vessel

A bioresorbable stent contains nineteen rings and three beams between each pair of rings.

The positions of the three beams alternate between each pair of rings. The geometry of the stent is built based on these characteristics of its shape.

The geometry of the stent and the vessel, in the STL file format, represents the physical boundaries in which the boundary condition of the partial differential equations locates. They represent the boundary of the vascular walls and the stents in three-dimensional form. The inflow and outflow ends of the vessel are a cross-section of the vessel perpendicular to the vascular wall. Since there is no physical interface on the cross-section at the two ends, we build “artificial” boundaries in order to prescribe the partial differential equation problem.

Mesh files in this project is produced by an automatic 3d tetrahedral mesh generator, called Netgen[4]. The geometries described in the previous section are loaded by Netgen as input files. The level of fineness of the meshes can be customized. Based on the capability and efficiency of our computing resources, the level of fineness is selected as "very fine" to keep the number of nodes (points) under 8000 and of elements under 30,000.

[4] http://sourceforge.net/projects/netgen-mesher/

3.2 LifeV

In order to solve the CFD problems that raised in our project, a scientific computing tool, named "LifeV" was adopted.

LifeV is a C++ software with an open source library of algorithms and data structures for the numerical solution of partial differential equations, distributed under the LGPL license. The development and maintenance of LifeV involves an international collaboration of universities and research institutions in Europe and the United States, including but not limited to the Politecnico di Milano (Italy), the École Polytechnique Fédérale de Lausanne (Switzerland), and Emory University in Atlanta (USA). This piece of software has been used for over a decade. The version employed in our project is its latest release, LifeV.

LifeV implements Galerkin finite element methods for solving partial differential equations, as well as a set of solvers for specific applications, including the Navier-Stokes solver.

Finite Element Method (FEM) has been validated that it is able to transfer the original problem to a numerically approachable problem with acceptable loss of accuracy (Passerini et al).

LifeV is compatible with different mesh files as part of the input, generated by Netgen or GMesh. The mesh generator utilized in our project is Netgen, which will be demonstrated in the next section. LifeV is capable of importing different mesh formats, such as the ones generated by Netgen and GMesh and it relies on visualization software such as ParaView.

3.3 The visualization software: ParaView

ParaView is an open-source, multi-platform data analysis and visualization application. ParaView users can quickly build visualizations to analyze their data using qualitative and quantitative techniques. The data exploration can be done interactively in 3D or programmatically using ParaView's batch processing capabilities.

ParaView was developed to analyze extremely large datasets using distributed memory computing resources. It can be run on supercomputers to analyze datasets of exa-scale size as well as on laptops for smaller data.[5]

In this study, ParaView is used to visualize the simulation and display the Wall Shear Stress

[5] http://www.ParaView.org/

(WSS) and Velocity in a dynamic fashion. The WSS in the last three seconds was represented in different colors based on the numerical value of the WSS and changed dynamically in time step of 0.1 second.

3.4 The environment in which the computation is conducted

The computation by WSS, speed and pressure is operated on two servers (cluster of servers) owned by Emory University, named Kinbote and Cheetah. Kinbote contains eight cores, each of which has eight processors. Cheetah, on the other hand, is cluster of 16 servers. The computation done by LifeV is conducted on Cheetah. The jobs typically took four servers and occupy all 8 processors on each core. Each job was assigned on the occupied servers and processors. Thus, the output was split into 32 pieces and would be merged afterwards. The Wall Shear Stress (WSS) defined in the previous section was only computed after the results were merged.

The department maintains a high performance cluster, Cheetah, with 32 nodes and 128 processor cores. Each node has two dual core AMD 2214 2.2 GHz Opteron CPUs, 4 GB RAM and an 80 GB drive. The nodes are connected via a High Performance InfiniBand network and

also Gigabit Ethernet. The nodes are running Linux CentOS. The cluster is managed by a head node, running Rocks, and it is using the Portable Batch System to schedule jobs.[6]

The department also maintains a parallel computing cluster, Kinbote, with 32 CPUs and 16 GB of memory split across 16 identical systems. All nodes use RedHat Linux/Intel for their operating system. Nodes are interconnected with switched, 100 MB Ethernet. Two build environments are available for MPI programs. One uses the GNU compiler suite [gcc/g++/g77]; the other uses the Portland Group (PGI) compiler suite.[7]

Output files are securely remote-copied from Cheetah to Kinbote, in which the merging process and computation of WSS were performed. The output CASE format files, compatible with the visualization software ParaView, were produced in this process.

[6] http://www.mathcs.emory.edu/

[7] http://www.mathcs.emory.edu/

4. Numerical Tests

4.1 Process

This project tests how blood flow behaves in straight and curved vessels at three stages of stent-adsorption. Stage 1 illustrates a full stent in a vessel before it starts to resorb, stage 2 demonstrates a stent in a vessel that has partially resorbed, and Stage 3 examines a vessel with a completely resorbed stent. Because the stent is gone, there is only a vessel in Stage 3 (see Figure 3) .

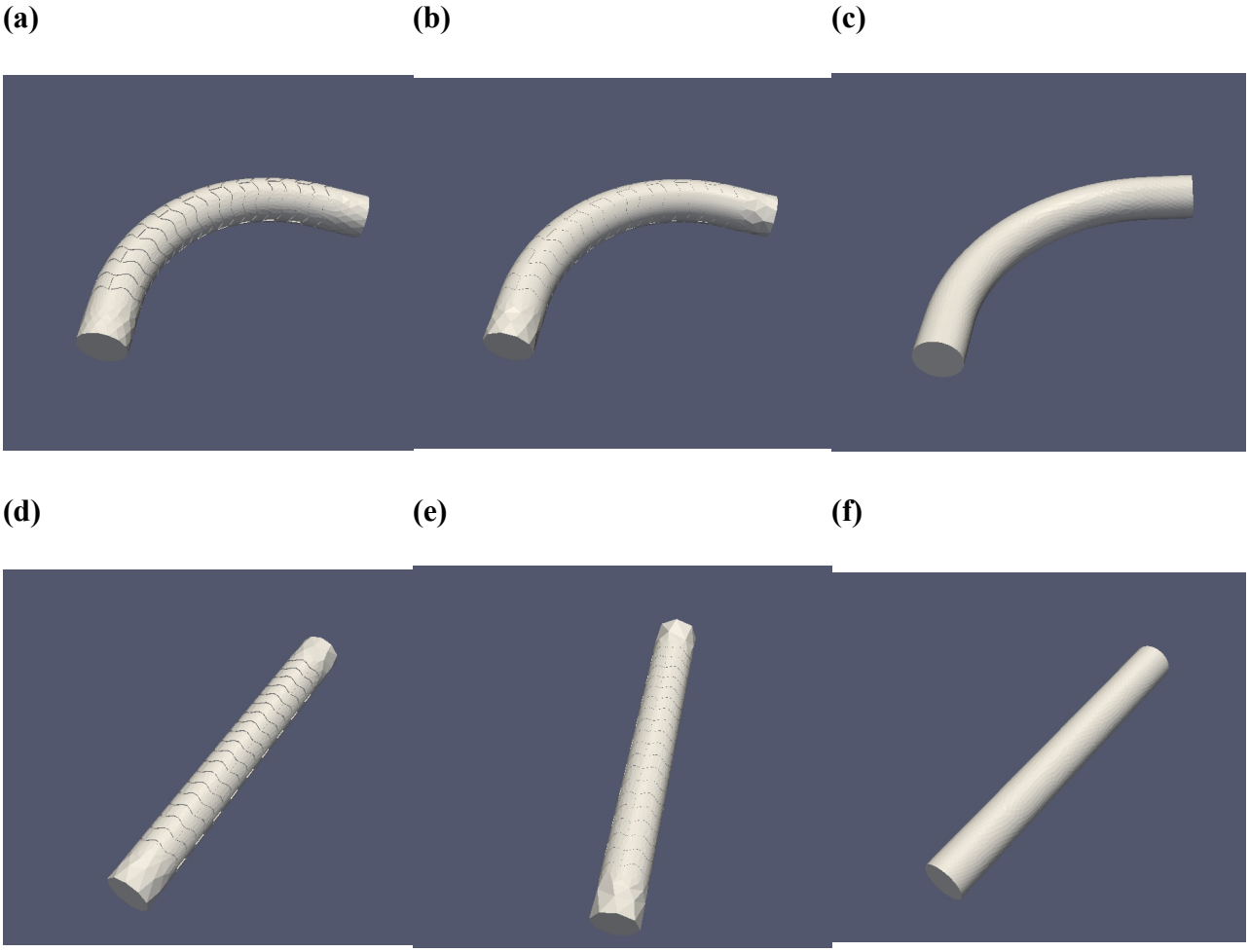

Figure 3. The six types of geometry[8]

The geometry files of the models are produced via Rhino. The vessel, as demonstrated in the previous section, is modeled as a segment of an infinite, hollow, rigid cylinder, straight and curved for the two cases in each stage. The stent is modeled true to its description and size. The stent in a curved vessel is conformed to fit the vessel, with the assumption that the stent can be

[8] (a) Curved vessel in Stage 1, (b) Curved vessel in Stage 2, (c) Curved vessel in Stage 3, (d) Straight vessel in Stage 1, (e) Straight vessel in Stage 2, (f) Straight vessel in Stage 3.

fully conformed, as the curvature of the vessel requires.

The geometry files are then processed by Netgen to produce mesh files in VOL format. Netgen meshes the files in this project with triangular interfaces. The smaller the sizes of the interfaces are, the finer the mesh output is. However, the fineness of the mesh output is not even across the entire structure. The surface of the vascular wall is meshed less coarsely than the interior of the vessel, since the wall is the focus in this project.

LifeV then takes a mesh file and the file containing patient-specific data as inputs. The later is used to prescribed boundary condition at the inflow end of the vessel. The duration of interest is five seconds after the starting point. As demonstrated in previous sections, LifeV will solve the Navier-Stokes equation for the velocity of blood flow and the pressure applied by the blood flow at any point of the interior of the blood vessel. The time step of computing and saving the output can be customized. In this project, computation is done every 0.01 seconds and output is saved for every ten computation-steps, which is 0.1 seconds.

In this project, LifeV runs parallel in a cluster of computers, called Cheetah (for detailed technical description, see Section 3.4). The jobs in this project are distributed to four servers in a

cluster via a script that can be executed in Linux environment. After the computation is done, the script then collects all output files from the four servers, brings them to the head server, and cleans up the rest of the servers after itself. The record of executing and error notes are stored separately and piped into two plain text files. If any error occurs during the process of executing or the job is accidently quitted, the two records can tell the user what happened.

Since the computation is conducted in four servers, each with eight processors, the result CASE file contains 32 pieces. To make the past-calculation processing easier, the result is merged to one piece by executing another script. The WSS is computed based on the result file, containing pressure and velocity. This step can be done using either the original 32-piece result files or the merged file. The merging process and calculation of WSS are done in a server, called Kinbote (for detailed technical description, see Section 3.4). The two jobs typically occupy one node in Kinbote.

The next step is to visualize the output files. The output mode of LifeV is designed to be compatible with the visualization software, ParaView. ParaView can show the pressure, velocity and WSS in different color based on the magnitude, and also play animation of these indicators

for the duration of interest.

4.2 The Visualization Results and Interpretation

The visualization results containing pressure, velocity and WSS are organized into six cases that involve stents in two different types of vessels and three stages of stent-absorption absorption. The pressure at the peak systole (3.5 second) and peak diastole (3.9 second) can be seen in Figure 4 and Figure 5, respectively.

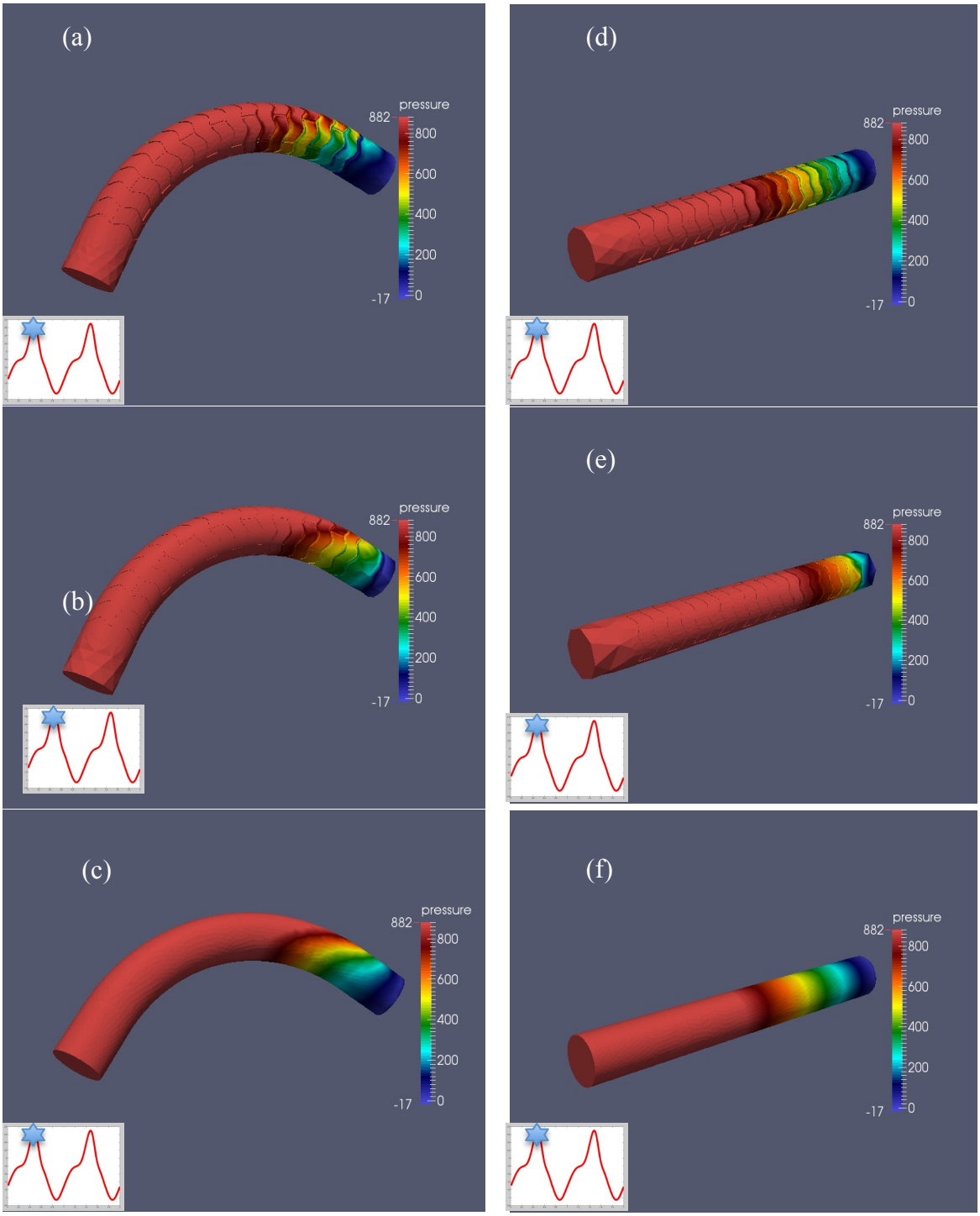

Figure 4. Pressure at the peak systole: (3.5 second) 8

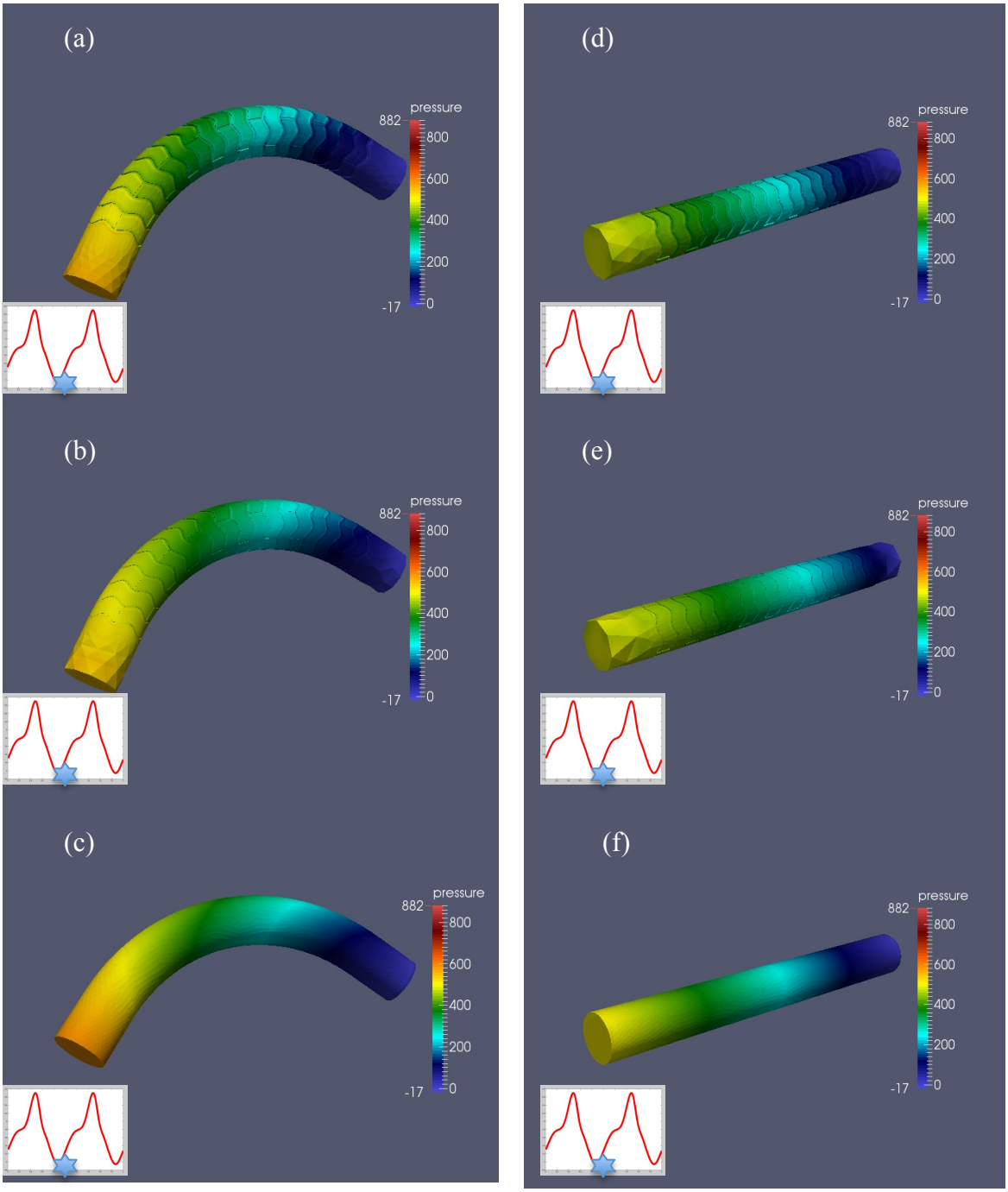

Figure 5. Pressure at peak diastole: (at 3.5 second)8

All the figures are scaled on the same range, from -17 to 882. As the figures indicate, pressure decreases from outer side of the arch to the inner side in the curved vessels and from inflow to outflow in both types of vessels. The outer side of the arch in the curved vessel may experience more impact than the inner side as the blood flows in. Moreover, the full stent raises the pressure of the blood between two rings of the stent, but decreases the pressure of the blood in the vicinity of the rings. The impact on the wall will be better demonstrated by the WSS.

The magnitude of velocity at the peak systole (3.5 second) and peak diastole (3.9 second) can be seen in Figure 6 and Figure 7, respectively.

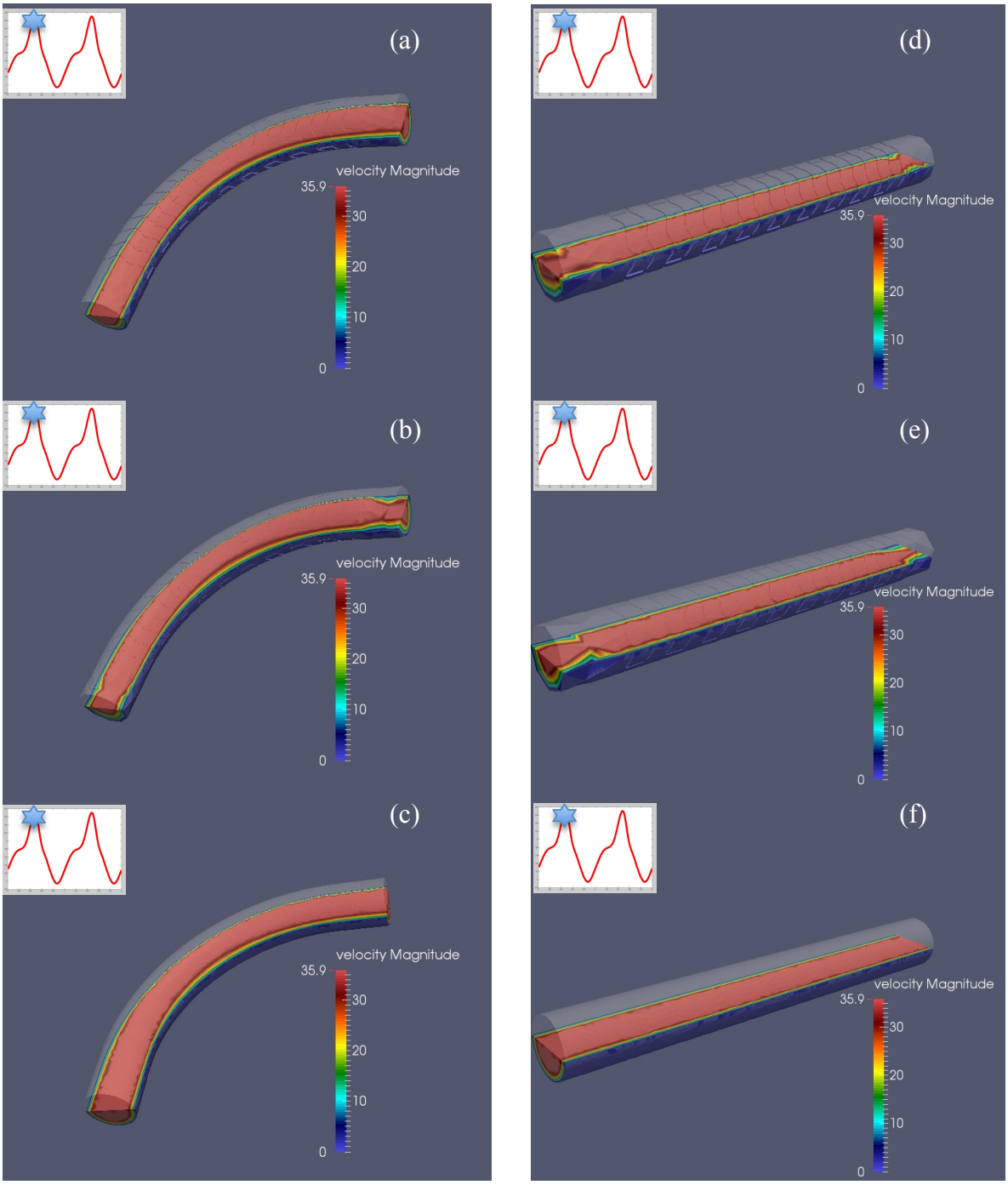

Figure 6. Magnitude of velocity at the peak systole: (3.5 second)8

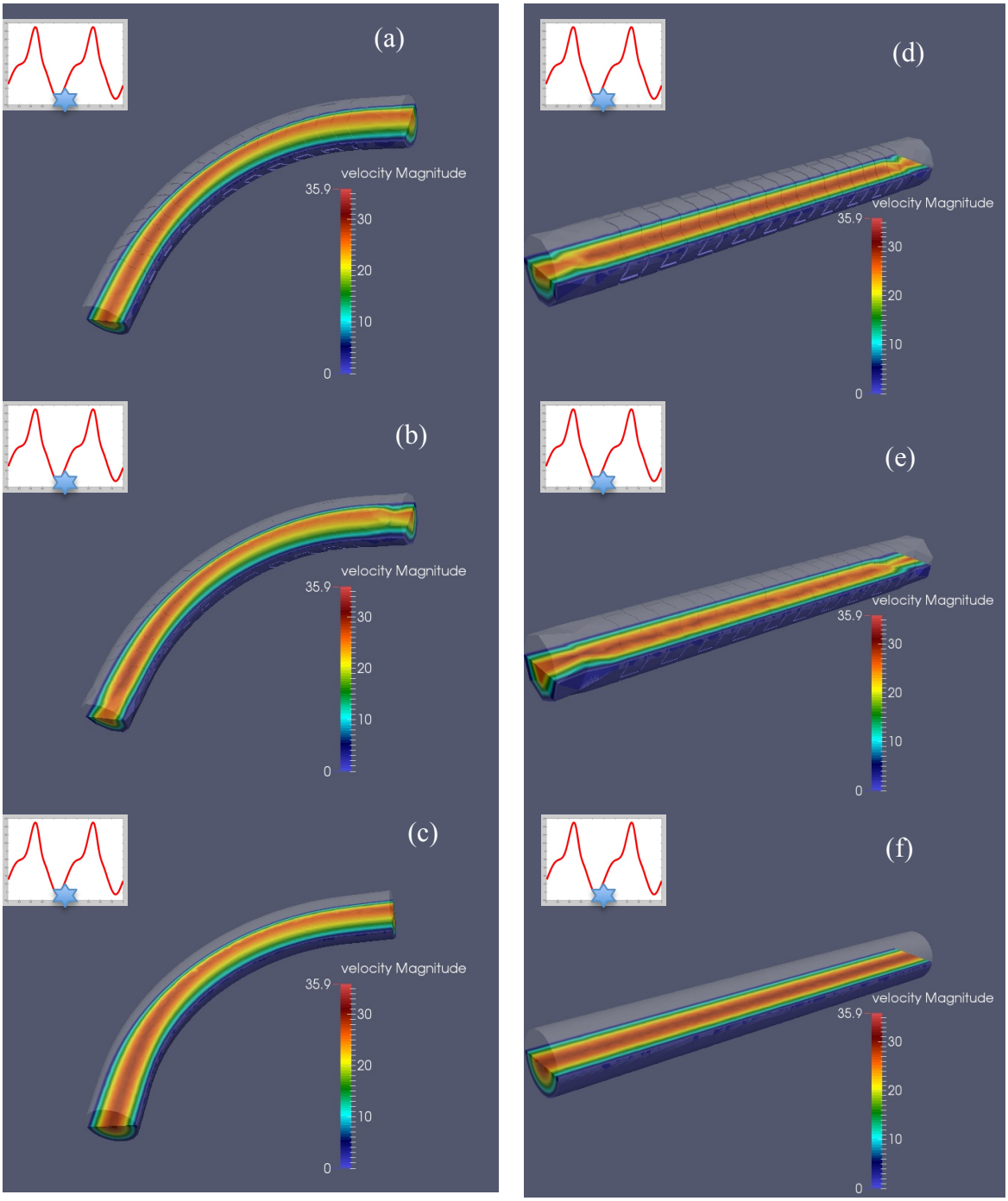

Figure 7. Magnitude of velocity at peak diastole: (at 3.9 second)8

One can observe that the highest value of the velocity magnitude is not at the center of the curved vessels. It is close towards the outer side of the arch in the curved vessel. Such phenomenon is called “Jet Effect”. Again, Jet Effect implies more impact from the blood flow to the arch. In addition, the center of the range approaches the outer side of the arch as the BVS is resorbed (from Stage 1 to 3, gradually). This could be a very interesting biomechanical influence from the BVS. One potential interpretation is that the resistance of BVS struts decreases as the BVS absorbs.

This unsymmetrical distribution also indicates that the motion of the blood flow could be more complicated than in straight vessels. The pattern of the blood flow motion can be better modeled by the streamlines of the blood flow.

The streamlines in the curved and straight vessels (3.8 second in stage 2) can be seen in Figure 8.

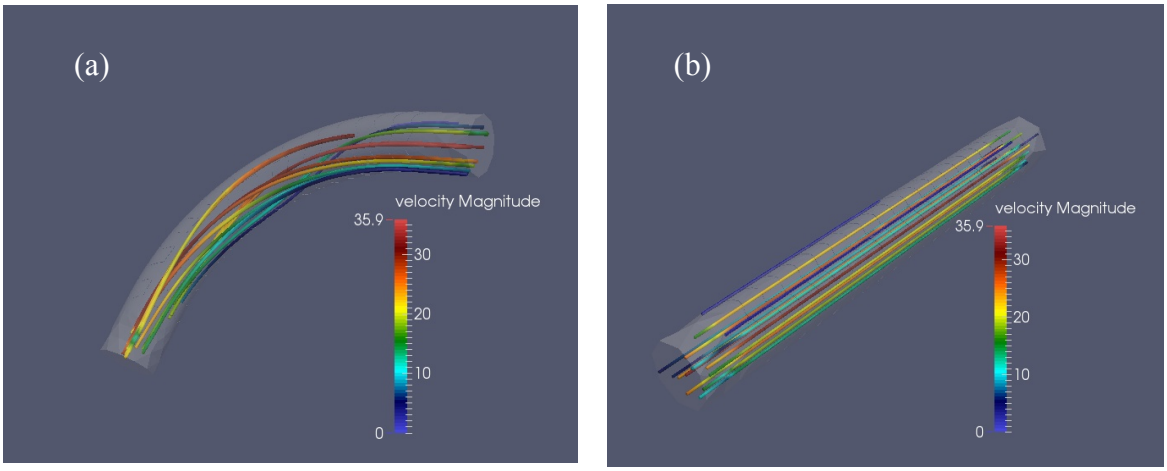

Figure 8. Streamlines of velocity in curved and straight vessels at Stage 2

The streamlines are colored based on their velocity. Both figures are scaled the same, from 0 to 35.9. One can observe that the blood tends to flow in a one-directional parallel fashion in the straight vessel, while it rotates and swirls in the curved vessels. The behavior of the blood flow in the curved vessel could be a very interesting aspect in the fluid dynamics of the blood and could indicate more impact on the outer side of the arch vessel.

With this type of model, one can visualize the motion of blood in the region of interest. One possible cause could be the motion of blood in the vicinity of the BVS struts. As Section 1.2 demonstrates, thicker struts may lead to potential formation of vortexes near the strut. The cross-section views of streamlines (3.9 seconds, the peak diastole) near the vascular wall for the straight vessels in the three stages of adsorption are shown in Figure 9.

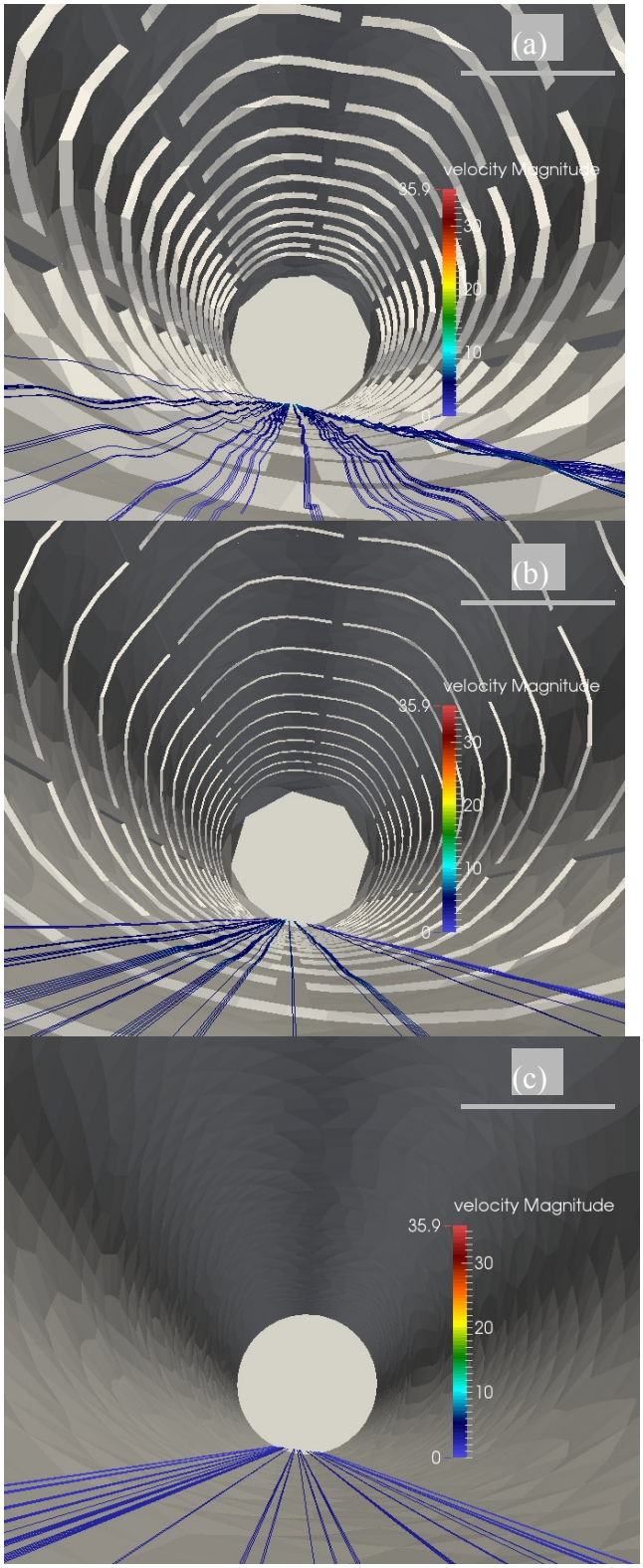

Figure 9. Velocity streamlines in straight vessels: (a) at Stage1, (b) at Stage2, (c) at Stage 3

There are minor waves in Stage 1 with matching patterns of the BVS structure that indicate the impact of the BVS. Very few waves can be seen in Stage 2 and none is observed in Stage 3. However, due to the fineness of the mesh, the figures might be too coarse to show any potential formation of vortexes if its range is even smaller than the mesh step size. This possibility will be discussed in more detail in the next section.

Another numerical indicator of interest is WSS. WSS was computed for only the last two seconds of the simulation, in order to obtain a realistic initial condition from the computation of the first three seconds. The WSS at the peak systole (3.5 second) and peak diastole (3.9 second) can be seen in Figure 10 and Figure 11, respectively.

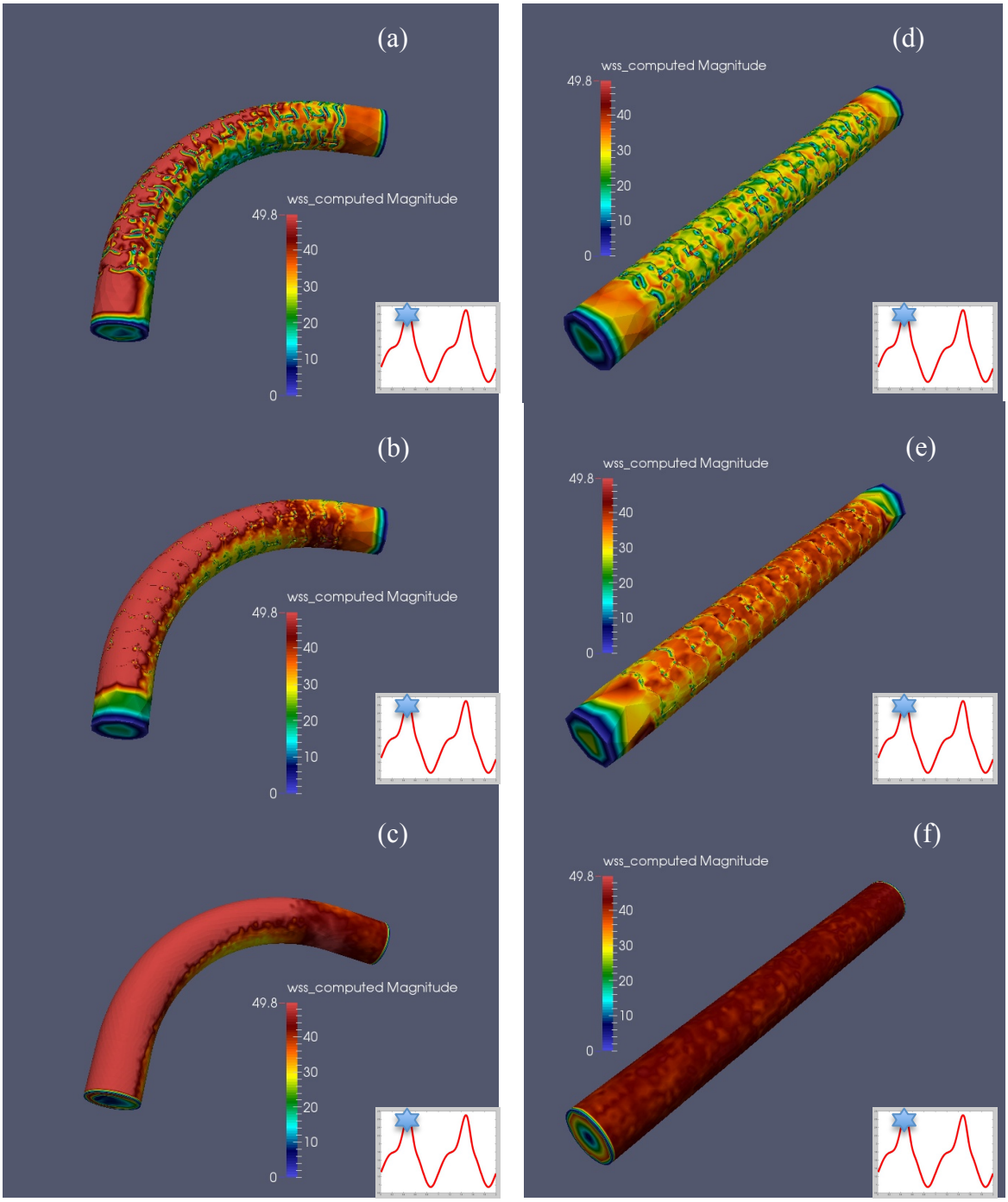

Figure 10. WSS at the peak systole: (3.5 second)8

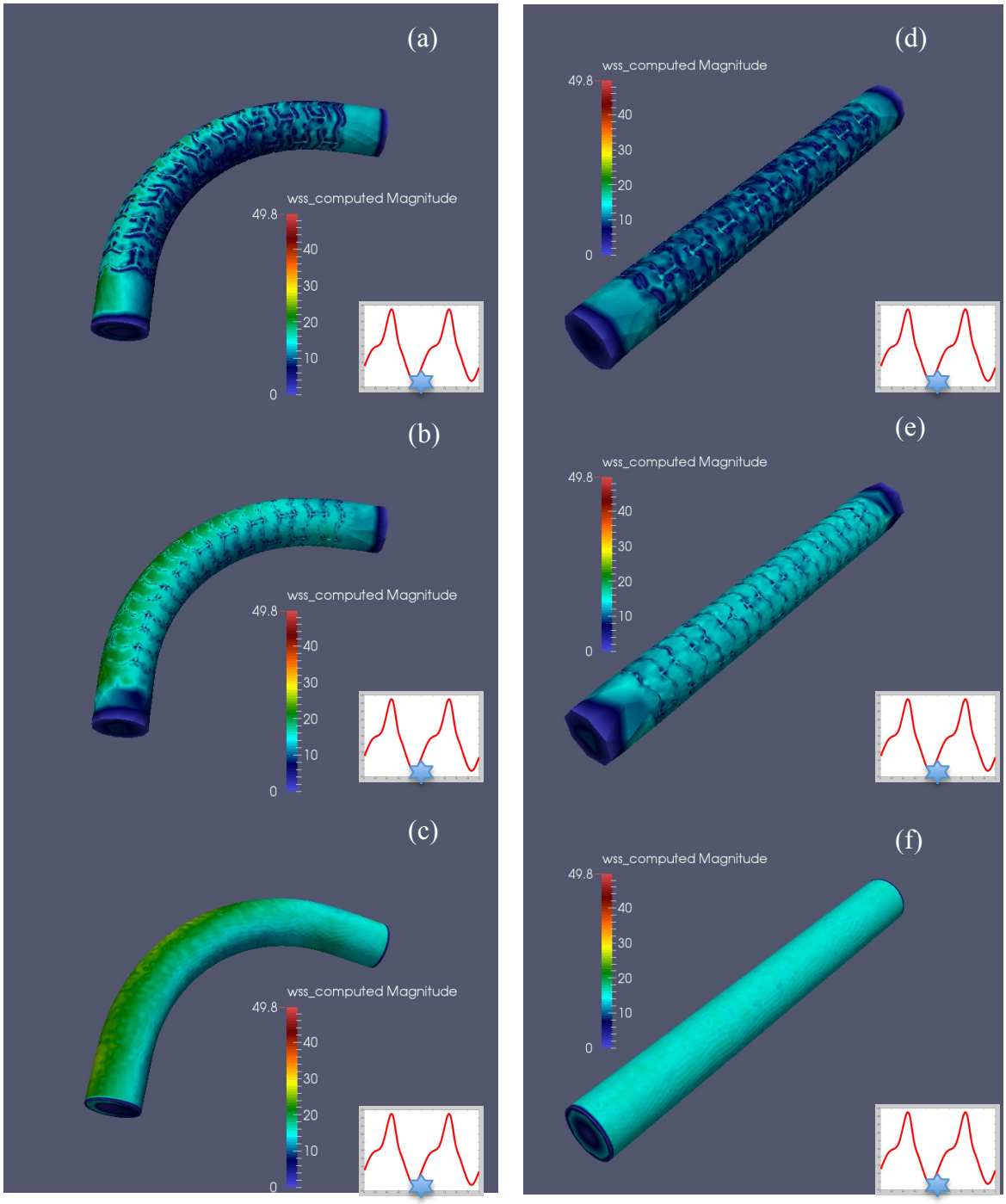

Figure 11. WSS at peak diastole: (at 3.9 second)8

In all three stages, the WSS in the close vicinity of the BVS is significantly decreased, while WSS in the region between any pair of the BVS rings increased. If one compared the WSS in corresponding locations in all three stages while the type of vessel remained the same, the pattern of WSS decreasing in the vicinity of BVS strut and increasing between any pair of BVS rings is less obvious as the BVS absorbed, Hence, it is reasonable to propose that BVS may polarize the WSS.

Through this study's figures of different types of vessels, one has a clear picture about the impact of blood flow on the outer side of the arch in the curved vessel. The WSS on the outer arch is significantly high at the peak systole. It is still slightly higher than the WSS of the inner arch at the peak diastole. High WSS indicates strong impact on certain regions of the vascular wall. The visualization of WSS matches the effect proposed by the unsymmetrical distribution of velocity magnitude and the rotation motion of the blood flow streamlines. It may alarm people that polarized WSS on the outer arch of the curved vessel, where the WSS is expected to be high regardless of the implants of BVS, may weaken that area of vascular wall or even make it vulnerable.

4.3 Discussion

Computational Fluid Dynamic has been widely used in numerical simulations of blood flow problems. The simulation process could be very complicated when the nature of blood flow and vascular wall are taken into consideration. The computation power required by such projects may vary, depending on their assumption. As section 2.1 and 2.2 demonstrated, blood flow is non-Newtonian fluid, due to its pulsatility and rheology. The vascular wall is elastic and changing in length during the cardio cycles. These natures of blood flow and vascular wall would largely complicate the mathematical model and require considerable amount of computational power and time, which often time is not available or accessible for the researcher. In this project, in order to accomplish six test cases with limited time and publicly shared resource of servers for computation, the blood flow is assumed to be Newtonian fluid, which allows the employment of Incompressible Navier-Stokes equation (INS). The vascular wall is assumed to be rigid and no blood is slipping in contact with the wall, which contributes to an approachable boundary condition.

Patient-specific data is employed for the modeling of blood flow, but not for the vessel wall. The reason we choose patient-specific data for blood flow is that, as section 1.4 demonstrated, the focus of this project is more of the fluid behaviors rather than the structure. Moreover, to collect patient-specific data of the vascular wall could be time-consuming. Since it has not yet been collected and made accessible for this project, to employ this type of data may not be approachable. In addition, the idealized model of the blood vessels in this project may have advantages over the patient-specific models. The idealized could allow one to investigate the influence brought executively by the BVS without other factors of the structure, including but not limited to the vascular wall motion, to bias the result or distract the investigation.

Despite the insights of this project, one should take its limitations into consideration. The mesh files of the computation are very coarse, so the simulation results may not be sufficiently accurate to justify the hypothesis. For instance, medical professionals and mathematicians have proposed that potential formation of vortexes may occur behind the strut of BVS due to its thickness (McDaniel and Samady 800). Simulations with finer meshes may provide a more precise result. Two simulations with meshes in different qualities are shown in Figure 12.

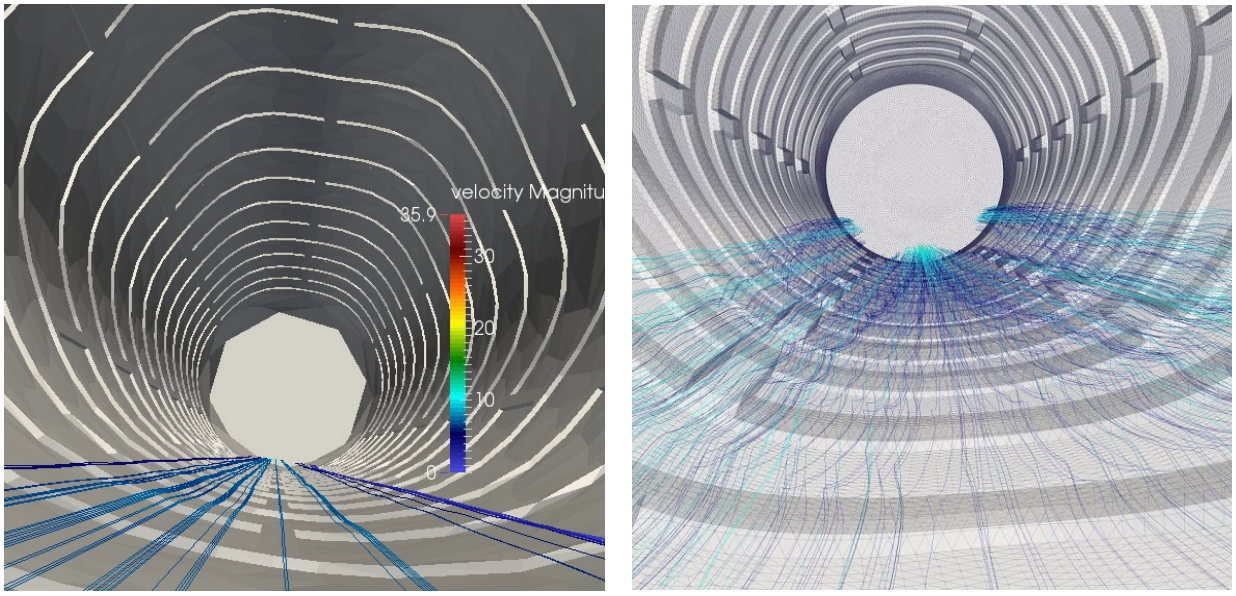

(a) (b)

Figure 12. Simulations with meshes in different quanlity

(a) Simulation with coarse mesh. (b) Simulation with fine mesh

In this pair of figures, the one with higher-quality shows smoother streamlines, while the other has clear trace of interpolation between the nodes. It's possible that the shape of potential formation of vortexes is even smaller than the edge of the mesh, so one cannot observe the potential formation of vortexes on the simulation figures.

4.4 insights

The visualization of numerical results in this project suggests but fails to strongly prove one

possible concern about the BVS, the potential formation of vortexes behind the stunt. Demonstrated in section 4.1.2, the WSS is low in the vicinity of the strut but high in the region between the ring struts. This distribution pattern of the WSS suggests there is a possibility that the blood flow may be turbulent behind the strut, but no obvious circulate streamlines of blood flow are observed in the velocity streamline figures. Due to the absence of visualized evident, this project fails to reject the hypothesis that no potential formation of vortexes exists. However, one cannot conclude that no potential formation of vortexes exists either, as the absence might be caused by the coarseness of the meshes.

One possible proposal of future study may be simulate the test cases with sufficiently fine meshes, if extraordinary computation power is available. Simulations with finer mesh (smaller edges) may provide more insights about the blood flow motion near the strut.

Another potential path of continued study would be to have the vascular wall more involved in the study of fluid-dynamic influence from the vascular wall. This approach is two-folded. For one, patient-specific data of the vascular wall can be taken into consideration, if it is collected and made accessible for the research team and bias from the data can be managed or separated

from the question. The potential bias could stem from the error of measurement when the data is being collected, system error of the equipment being employed and factors whose strong affect overcomes that of the stent. For the other, the vascular wall could be modeled dynamically, in which case the features of vascular wall motion can be considered.

Reference

Abbott. *Absorb Bioresorbable Vascular Scaffold*. Abbott Laboratories, 11 Jun. 2013. Web. 13 March 2014. ‹http://www.absorbmediakit.com/absorb.htm›.

Batchelor, G. K. *An Introduction to Fluid Dynamics*. Cambridge: U.P., 1967. Print.

Ciechanowski, Stanislaus. *Anatomical Researches on the So-called "prostatic Hypertrophy" and Allied Processes in the Bladder and Kidneys*. New York: Pelton, 1903. Print.

Dennis O'Neil. *Blood Components*. *Palomar College*, 1999. Web. 13 March 2014. ‹ http://anthro.palomar.edu/blood/blood_components.htm›.

Eshtehardi P., M.C. McDaniel , J. Suo. "Association of wall shear stress with coronary plaque progression and composition: a serial human radiofrequency intravascular ultrasound study (abstr)." *Arterioscler Thromb Vasc Biol* (2010): 236. Print.

Eshtehardi, Parham, Michael C. McDaniel, et al. "Association of wall shear stress with coronary plaque progression and composition: a serial human radiofrequency intravascular ultrasound study (abstr)." *Journal of the American Heart Association* (2012): 236. Print.

Fung, YC, K. Fronek, P., and Patitucci. "Pseudoelasticity of arteries and the choice of its

mathematical expression." *American Journal of Physiology* (1979): 620-631

Galdi, GP, Rannacher R. Robertson AM, Turk S. *Hemodynamical Flows*. Delhi: Delhi Books Store, 2008. Print

Gogas, Bill D., Alessandro Veneziani, et al. "Biomechanical Assessment of Fully Bioresorbable Devices (abstr)." *JACC Cardiovascular Interventions* (2013): 760-761. Print.

Gray, Henry, F.R.S, H. V. Carter, and Robert Howden. *Anatomy, Descriptive and Surgical*. Ed. T. Pickering Pick. Fifteenth ed. New York: Barnes & Noble, 2010. Print.

J.J., R. Krams, J.C. Schuurbiers. "Relationship between neointimal thickness and shear stress after Wallstent implantation in human coronary arteries." *Circulation* (2001):1740-1745. Print.

Maton, Anthea, Roshan L. Jean Hopkins, Charles William McLaughlin, Susan Johnson, Maryanna Quon Warner, David LaHart, Jill D. Wright. *Human Biology and Health.* Englewood Cliffs, NJ: Prentice Hall, 1993. Print.

McDaniel, Michael C., and Habib Samady. "The Sheer Stress of Straightening the Curves: Biomechanics of Bioabsorbable Stents." *JACC Cardiovascular Interventions* (2011):

800-802. Print.

Papafaklis M.I., C.V. Bourantas, P.E. Theodorakis. “The effect of shear stress on neointimal response following sirolimus- and paclitaxel-eluting stent implantation compared with bare-metal stents in humans.” *J Am Coll Cardiol Intv*. (2010):1181-1189. Print.

Passerini, T., A. Quaini, U. Villa, A. Veneziani, and S. Canic. "Validation of an Open Source Framework for the Simulation of Blood Flow in Rigid and Deformable Vessels." *International Journal for Numerical Methods in Biomedical Engineering* 29.11 (2013): 1192-213. Print.

Pedley, T. J. *The Fluid Mechanics of Large Blood Vessels*. Cambridge: Cambridge UP, 1980. Print.

Schowalter, William Raymond. *Mechanics of Non-Newtonian Fluids*. Oxford, England: Pergamon, 1978. Print.

Skalak, Richard, and Shu Chien. "Static Elastic Properties of Blood Vessels." *Handbook of Bioengineering*. New York: McGraw-Hill, 1987. N. pag. Print.

Slawinski, Jaroslaw, Tiziano Passerini, Umberto Villa, Alessandro Veneziani, and Vaidy

Sunderam. “Experiences with Target-Platform Heterogeneity in Clouds, Grids, and On-Premises Resources.” *Parallel and Distributed Processing Symposium Workshops & PhD Forum (IPDPSW) 2012 IEEE 26th International* (2012): 41-52. Print.

Stone P.H.. “The PREDICTION Trial: in-vivo assessment of coronary endothelial shear stress, arterial remodeling, and plaque morphology to predict coronary atherosclerosis progression and rupture in man.” 10 April 2014. <http://www.tctmd.com/show.aspx?id=105491>

Veneziani, Alessandro. " Mathematical and Numerical Modeling of Blood Flow Problems." PhD thesis. University of Milan, 1998. Print.